Available online at www.sciencedirect.com
ScienceDirect
Journal of the European Ceramic Society 28 (2008) 3165–3176
www.elsevier.com/locate/jeurceramsoc

Oxidation of titanium carbide–graphite hetero-modulus ceramics with low carbon content
I. Phenomenological modeling of the ridge effect

Igor L. Shabalin [a,*], Daniel L. Roach [a], Leonid I. Shabalin [b]

[a] *Institute for Materials Research, The University of Salford, Greater Manchester M5 4WT, UK*
[b] *Russian State Professional and Pedagogical University, Yekaterinburg 620012, Russia*

Available online 25 June 2008

Abstract

Hetero-modulus ceramic composite materials (HMC) present an opportunity to combine a ceramic matrix having high Young's modulus with inclusions of a material having a considerably lower value of Young's modulus, resulting in a material with significantly improved properties. The isobaric–isothermal oxidation of 93 vol.% TiC–7 vol.% C (graphite) hot-pressed HMC was studied at temperatures of 400–1000 °C and pressures of 0.13–65 kPa in oxygen flow using a microbalance. The TGA data and carbon content analysis of oxidised samples were applied in the kinetics phenomenological modeling for both carbon burn-off and oxygen consumption processes. The activation energies Q and orders of reaction m were determined for all oxidation parameters and stages of the process, described using a linear–paralinear model. The oxidation behaviour of the material is characterised by the presence of a so-called "ridge effect". The ridge temperature and ridge oxygen pressure serve as boundaries between regions defined by higher or lower values of oxidation parameters and mark a change in the prevailing oxidation mechanism, as while traversing the ridge parameter the values of Q and m change their sign.

Keywords: Composites; Chemical properties; Carbon; Hetero-modulus ceramics; TiC

1. Introduction

Hetero-modulus ceramic composite materials (HMC) present the combination of ceramic matrix having high Young's modulus (300–600 GPa) with inclusions of a dispersed high-temperature phase having significantly lower Young's modulus (15–20 GPa) such as sp^2-structured graphite or graphite-like, hexagonal boron nitride. Subsequently it becomes more effective to use brittle refractory compounds (carbides, oxides, nitrides, borides and silicides) with the highest melting points in the most modern high-temperature engineering applications. The generally low thermal shock resistance of these brittle materials with high elastic moduli can be greatly improved by the addition of low-modulus phases. Similar materials, successfully applied in rocket and spacecraft design were referred to as "high-E–low-E composites" in the USA[1,2] and "hetero-modulus ceramics" in the USSR, Russia and Ukraine.[3–7] Also known as "soft ceramics" to emphasise another great advantage of HMC, namely the remarkable machinability by conventional tools with a high grade of accuracy[6] that is not normally feasible with conventional ceramics. The experience gained through the application of HMC was subsequently shifted from space and nuclear technologies to metallurgy and machinery as HMC provide significant engineering opportunities.[4–6] One of the types of HMC, in particular the refractory transition-metal carbide–carbon composites,[3–4,7] are prospective materials for a number of high-temperature applications: as thermally stressed components of solid and liquid propellant rocket engines, elements of thermal protection for re-entry spacecraft, diaphragms for casting metallurgical equipment, highly loaded brake-shoes in aviation and automobile engineering, high-temperature lining and heating elements and others, including TiC–carbon composites, which (because of the relatively low Z of components) are real candidates for thermonuclear fusion reactors as a plasma facing material.[8]

If the scales formed on the HMC during high-temperature gas exposure possess protective properties and prevent corrosion propagation, the chemical stability of carbide–carbon HMC

* Corresponding author. Tel.: +44 161 295 3269; fax: +44 161 295 5575.
E-mail address: i.shabalin@salford.ac.uk (I.L. Shabalin).

0955-2219/$ – see front matter © 2008 Elsevier Ltd. All rights reserved.
doi:10.1016/j.jeurceramsoc.2008.04.035

Table 1
Oxidation kinetics of different materials based on titanium carbide

Material (composition, manufacturing method)	Gaseous reagent	Gas pressure (kPa)	Temperature (°C)	Kinetics character	Activation energy (kJ mol^{-1})	Reaction order	Reference
TiC_{1-x}, hot-pressed	Air	~100	600–1100	Parabolic	–	–	[12]
TiC_{1-x}, $x = 0.97$; 0.63, sintered (97%)[a]	O_2	~100	900–1000	Parabolic (approximately)	–	–	[13]
TiC_{1-x}, sintered (96%)[a]	O_2 (flow)	~100	300–450	Linear	–	–	[14]
			450–700	Linear, parabolic (approximately)	–	–	
			700–1000	Parabolic (approximately)	–	–	
TiC_{1-x}, powdered	O_2	0.8–86	600–800	Parabolic	190	1/6	[15]
			800–900	Parabolic	190	1/4	
TiC_{1-x}, single crystal	O_2	86	900–1000	Parabolic (approximately)	–	–	
TiC_{1-x}, $x = 1.00$, single crystal	O_2, O_2/Ar	0.01	1015	Linear	150 ± 8	1/2	[16]
		1.3–40	815–1215	Parabolic	205 ± 8	1/2	
		96	690–1015	Parabolic (with deviation to linear)	–	–	
TiC_{1-x}, $x = 0.94$[b], hot-pressed (97%)[a]	O_2	0.01–98	700–900	Paralinear	26 ± 3 (parabolic)[b], 300 ± 30 (linear)[b]	–	[17]
			900–1200	Paralinear	310 ± 30 (parabolic)[b], 135 ± 3 (linear)[b]	1/2 (parabolic)[b], 1/3 to 1/4 (linear)[b]	
TiC_{1-x}, $x = 0.97$, powdered	O_2/Ar	3.9–16[c]	350–420	Parabolic (4 steps)	125–150	0.2–0.6	[18]
			420–450	Parabolic (4 steps)	42–71	–	
TiC_{1-x}, $x = 0.97$, powdered	O_2/Ar	2–60[c]	300–900	Parabolic (4 steps)	–	–	[19]
TiC_{1-x}, $x = 0.96$, single crystal	O_2/Ar	0.08[c]	700–1500	Contracting volume equation	–	–	[20]
$(Ti_{0.5}Hf_{0.5})C_{1-x}$, $x \sim 1.0$, hot-pressed (99%)[a]	O_2/Ar	0.08[c]	1200–1400	Parabolic	–	–	[21]
TiC_{1-x}, $x = 0.97$, powdered	O_2/Ar	5/95	300–400	Parabolic (3 steps)	~200	–	[23]
	O_2/H_2O/Ar	5/5–10/90	300–400	Parabolic (3 steps)	~140	1/2(H_2O)[d]	
	H_2O/Ar	5–15/95	520–650	Parabolic (3 steps)	~180	–	
TiC_{1-x}, HIPed	O_2/Ar,	5/95	900–1200	Paralinear	–	–	[24]
	O_2/H_2O/Ar	5/5/90	900–1200	Paralinear	–	–	
	H_2O/Ar	5/95	900–1200	Paralinear	–	–	
TiC_{1-x}, HIPed (>98%)[a]	O_2/Ar,	5/95	850–1200	Paralinear	–	–	[25]
	O_2/H_2O/Ar	5/5/90	850–1200	Paralinear	–	–	
	H_2O/Ar	5/95	850–1200	Paralinear	–	–	
TiC_{1-x}, $x = 0.97$[b], sintered	O_2/Ar	0.01–0.02[c]	745–1050	Linear (with deviation to parabolic)	180 ± 10	–	[26]
TiC_{1-x}, $x = 0.97$[b], sintered	O_2/Ar	0.0008–0.02[c]	665–1045	Linear (with deviation to parabolic)	158 ± 2	−3/4[b]	[29]
TiC_{1-x}, $x \sim 1.0$, hot-pressed and annealed (>98%)[a]	Air	~100	600–700	Logarithmic			[40]
			700–1200	Parabolic			
TiC–C, hot-pressed (97%)[a]	O_2	1.3–13	500–1000	Parabolic (mainly)	–	–	[3]
(Ti, Cr)C–C, fused	Air	~100	1000–1550	Linear (mainly)	–	–	[36]

[a] Relative density in percents with theoretical.
[b] Calculated from the experimental data.
[c] Partial pressure of O_2.
[d] Related to the partial pressure of H_2O.

in active gaseous and melt media, the resistance to corrosion will become significantly higher than those for other high-temperature materials, e.g. carbon–carbon composites, which are currently widely used across a number of fields of engineering. Therefore, advanced HMC can provide an opportunity to increase the working temperatures and/or operational life times for components in highly technological systems (such as rocket propulsion assemblies). However, some previous physico-chemical studies have shown that, in general the formation of oxide scales on the transition-metal carbides as a result of surface oxidation does not generate an effective barrier for the inhibition of bulk oxidation.[9–11] The oxidation process on the carbide surface during oxygen exposure seems to be highly sensitive to temperature and gas pressure. Hence, first of all, knowledge of the kinetics of such a chemical interaction and development of models for this process should allow forming the corrosion-resistant scales. A coating of these scales on the working surfaces of carbide–carbon HMC components by means of preliminary oxidation of this material under strictly controlled conditions could prove to be most useful in protecting them from erosion by high-speed and high-enthalpy gaseous flows. Similar technique could also be of great relevance to the current processing technology of functionally graded materials developed over the last decade.

Interaction between carbide phase and oxygen only seems to be simple at a glance. Though the first oxidation kinetics studies of carbides, including titanium carbide, date back to the 1950–1970s,[12–17] even the prolific production of recent publications, mostly due to the works by Shimada et al.[18–25,30] and Gozzi et al.,[26–34] has not completely clarified some features of the oxidation kinetics for these compounds, as the data available in literature are not only differed, but sometimes, it is in contradiction with each other. Various models (linear, parabolic, logarithmic, etc.) were employed for oxidation of TiC (Table 1), though no one of them have tried to describe temperature and oxygen pressure relationships as well as their mutual influences on the process in extended ranges of the parameters. There are still some indeterminate problems especially connected with the role of carbon in oxidation of carbide phases, which, up to now, has not been well understood too.

Also it is necessary to note that the existing knowledge on oxidation of TiC cannot be applied without reservation, as the oxidation behaviour of carbide–carbon HMC is rather different to that of its individual components due to the mutual influence of the derived products on the oxidation process. Furthermore, the structures of the carbide phase in HMC formed at high temperatures in direct contact with excess carbon (especially the concentration of defects)[3,7] significantly differs from the structures of the hypostoichiometric phases traditionally used as individual carbides in physico-chemical experiments. It is also impossible to ignore the general influence of any carbon additives on the chemical activity of these composites, because the great variety of carbon components introduced using alternative methods lead to the fabrication of HMC with properties that are essentially different. Nevertheless, the studies of the oxidation of carbide–carbon HMC carried out with materials prepared by hot-pressing,[3] arc-melting[35,36] and impregnation of graphite[37] have revealed that carbide phase oxidation dominates the corrosion process of such composites. But these previous works had mainly estimated the relative corrosion resistance for the prepared samples of HMC without any treatment of the process itself. Therefore, the aim of this work is, while exploring the evolution of the oxidation process of HMC based on titanium carbide–graphite compositions with low carbon content, to establish and develop a general oxidation phenomenological/kinetics model, which could describe the influence of temperatures and oxygen pressures on the rate of the solid–gas interaction across a wide range of variation of these parameters, as well as to investigate better the behaviour of carbon in the oxidation process of TiC–C HMC in a whole.

2. Experimental

The carbothermic titanium carbide powders (KZTS, Russia) with a particle size 1–4 μm containing 78.5 wt% Ti, 19.6 wt% C, 0.7 wt% W, 0.5 wt% O, 0.4 wt% Fe, 0.1 wt% Co were used for the production of the HMC matrix and the powders of natural graphite marked YeUZ-M and standardised by GOST 10274-92 (KKZ, Russia) with mineral residue less than 0.1 wt% were used as a low-modulus component in this study. The densities of components determined by XRD were 4.90 and 2.25 g cm^{-3} for titanium carbide and graphite phases, respectively. The blanks of 93 vol.% TiC–7 vol.% C HMC were prepared by hot-pressing in graphite moulds at 2700 °C under an applied pressure of 12 MPa in protective atmosphere of pure argon. All details of the manufacturing method for the composite material and the microphotograph of its structure are given in our recent paper.[7] The physico-chemical characteristics of the studied HMC are reported in Tables 2 and 3.

The thermogravimetric analysis (TGA) of HMC samples was carried out using a somewhat modernised version of the installation described in the papers by Afonin et al.[38,39] This installation provided stable pressures in the range of 0.1–80 kPa

Table 2
Physico-chemical characteristics of 93 vol.% TiC–7 vol.% C (graphite) HMC

Material code	TKU-1
C/Ti	1.17
Composition (vol.%)	
TiC_{1-x}	93
C	7
Chemical analysis (wt%)	
Ti	74.7
C[a]	21.9
O	0.6
N	0.5
W	0.6
Fe + Co	0.3
Density	
g cm^{-3}	4.60
%[b]	97.5

[a] Total carbon content.
[b] Relative density in percents of theoretical density calculated from XRD measurements for the components.

Table 3
Physico-chemical characteristics of phases in 93 vol.% TiC–7 vol.% C (graphite) HMC

Material code	TKU-1
Phase analysis	TiC_{1-x}, C (graphite)
Titanium carbide	
Lattice parameter a (nm)	0.4326 ± 0.0001
Micro-hardness HV (GPa)	24 ± 1
Average grain size (μm)	75 ± 10
Graphite[a]	
Lattice parameter a (nm)	0.246 ± 0.001
Lattice parameter c (nm)	0.670 ± 0.001

[a] Lattice parameters before high-temperature hot-pressing: $a = 0.246$ nm and $c = 0.677$ nm.

with mass rate of oxygen flow of 60–160 mg min^{-1}. It was clearly evident that all TGA experiments provided stable oxygen content above the surface of the samples due to the independence of TGA results with respect to the fluctuations of flow rate. Before being fed into the reaction unit, oxygen was bled out through a special purification system. Possible contamination of the oxygen amounted to less than 0.01 wt%, and the accuracy of measurement for the employed TGA method amounted to 0.1% with threshold of sensibility—about 0.1 mg cm^{-2}. The HMC samples were shaped into plates with dimensions of 7 mm × 7 mm × 1 mm and weight of about 200 mg by cutting the hot-pressed ceramic blanks and subsequent polishing the surfaces with diamond tools. The cutting-off scheme for samples prepared for TGA was as shown in Fig. 1. About 80% of the oxidized surface of each sample was represented by the planes, which were parallel to the axis of hot-pressing; it was important as flake-like graphite inclusions in the hot-pressed material were oriented with their base planes preferably perpendicular to this axis. The monitoring of density was used to reject the samples with deviation more than 0.02 g cm^{-3} from average value (see Table 2). The sample surfaces before TGA were cleaned with ultra-sound in oxygen-free organic solvents (toluene and dichloroethylene) and dried in vacuum at room temperature for 12 h. All these cautions allowed to achieve the level of reproducibility for TGA curves up to 99.5–99.8%.

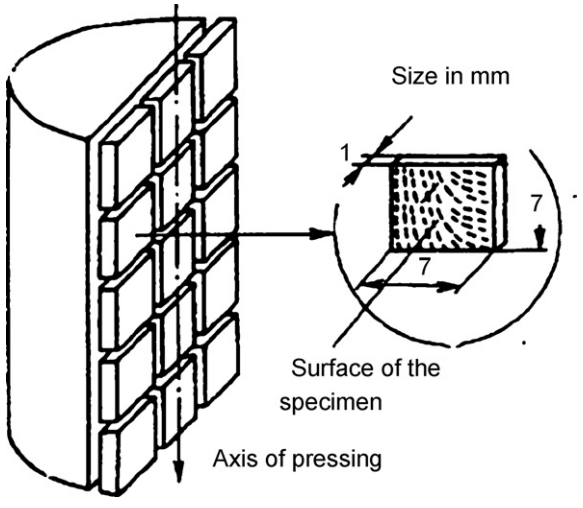

Fig. 1. The scheme for preparation the samples for TGA by cutting-off a blank of 93 vol.% TiC–7 vol.% C HMC.

The determination of carbon content in the oxidised samples was carried out using a coulometric method with a CuO–Pb flux employing a special analyser with the relative accuracy of measurement at about 0.2%. Additionally, good agreement was achieved between the results for carbon content determination and an experiment to convert the samples to the stoichiometric form of titanium dioxide, using complete burn-off of carbon in the samples at 900 °C in air for about 18 h.

3. Results and discussion

3.1. TGA kinetics

The isobaric–isothermal oxidation of 93 vol.% TiC–7 vol.% C (graphite) HMC was performed at temperatures of 400–1000 °C and pressures of 0.13–65 kPa in oxygen with mass flow rate of gas at the level of 120 ± 20 mg min^{-1}. No appreciable deviation in weight was observed at 400 °C, as the notable weight gain of the materials was only observed at temperatures of 500 °C for oxygen pressure of 1.3 kPa, 600 °C – for 0.65 kPa and 700 °C – for 0.13 kPa. The change of sample weight was normalised to the initial surface area of the sample and presented via plots showing weight gain per unit surface, w versus time, t; some typical results of the TGA obtained at different temperatures and oxygen pressures are shown in Figs. 2 and 3. The mathematical processing showed that the TGA curves for the HMC samples could be divided into three (or four) stages. In the initial stage ($0 < w < 5$ mg cm^{-2}), the oxidation process is almost linear with time, as it is shown in Fig. 4, and may be described by the following equation:

$$w = k_1 t + c_1 \quad (1)$$

where k_1 is the linear rate constant, and c_1 is an integration constant. The length of this stage is dependant on temperature and oxygen pressure; for example, at 1000 °C and 1.3 kPa the first stage of the oxidation process extends to 30 min, yet an equal temperature and greater pressure of 65 kPa results in a first stage of just 1 min. Subsequently, in the second-stage oxidation rate, w is best described by a parabolic function, such that

$$w^2 = k_p t + c_p \quad (2)$$

where k_p denotes the parabolic rate constant, and c_p is an integration constant. For the case of oxidation at higher temperatures/higher oxygen pressures ($T \geq 700$ °C and $p_{O_2} \geq 13$ kPa), this stage was followed by another parabolic stage, which is also described by the Eq. (2), giving rise to two parabolic stages with different constant coefficients. In the final oxidation stage, the oxidation process returns to a linear form similar to that found in the first stage, with reaction rate w given by Eq. (1), but with significantly decreased values for corresponding linear rate constant, $k_{12} = dw/dt$. The analogous behaviour was observed across the entire range of temperatures and pressures applied. Thus, for example, to describe the process at higher temperatures/higher oxygen pressures, one would apply two linear rate

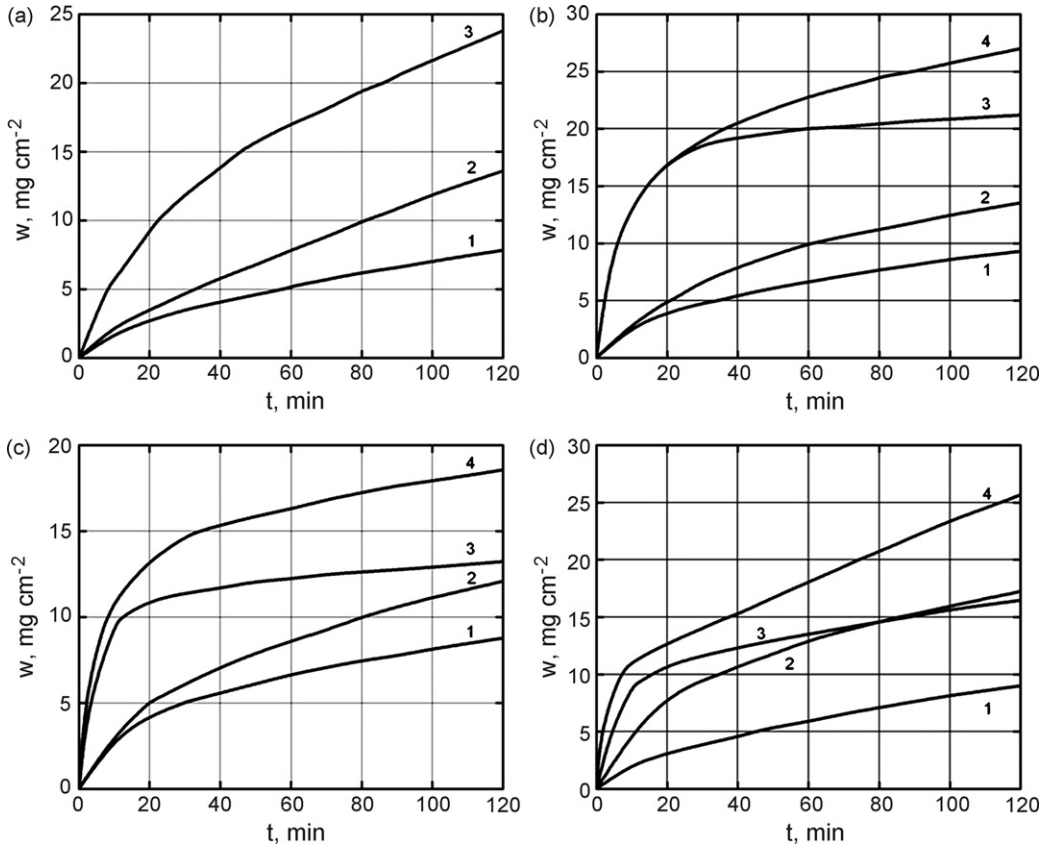

Fig. 2. The isobaric–isothermal oxidation TGA kinetics of 93 vol.% TiC–7 vol.% C HMC at different oxygen pressures, p_{O_2}: (a) 1.3 kPa; (b) 13 kPa; (c) 26 kPa; (d) 65 kPa for lower temperatures, T: (1) 500 °C; (2) 600 °C; (3) 700 °C; (4) 800 °C.

constants: k_{l1} and k_{l2}, and two parabolic rate constants: k_{p1} and k_{p2} (see Fig. 4b), however, for other regions defined by higher or lower values of oxidation parameters, the constants, which completely describe the oxidation behaviour of the material, are: k_{l1}, k_p and k_{l2} (see Fig. 4a).

The parabolic stages of the process take up the majority of the time with $1–10 < t < 30–100$ min and the weight gain equal to $1–5 < w < 5–25$ mg cm^{-2}, including the "second parabolic" stage, occuring for higher temperatures/higher oxygen pressures range with $10–17.5 < w < 12.5–25$ mg cm^{-2}. The second-linear stage began after 30 min of oxidation at 1000 °C and 65 kPa, while at 700 °C and 0.13 kPa the start of this stage occurred at 100 min. The specific weight gain, w connected with the beginning of the last stage of the process was quite different: from 2 mg cm^{-2} (1000 °C, 1.3 kPa) up to 25 mg cm^{-2} (800 °C, 13 kPa). Hence, the assembly of observed TGA curves for the oxidised HMC samples can be characterised comprehensively as a linear–paralinear model, whose main properties are in the alternation of linear and parabolic stages rather differentiated for the higher temperatures/higher oxygen pressures range.

It should be pointed out especially that there was no steady increase of weight gain from the lowest temperatures and pressures to the highest ones in the studied range of oxidation parameters. Indeed, within this range, there is a clearly defined maximum weight gain, which corresponds to particular values of the oxidation parameters, but that this maximum does not appear at the maximal temperature or oxygen pressure. Voitovich and Pugach[40] also found that quasi-stoichiometric hot-pressed TiC possessed the highest values of oxidation rate at 800 °C when studying oxidation in the range of temperatures between 600 and 1000 °C. However, the detailed phenomenological model for the oxidation kinetics of TiC–C HMC samples can be better visualised by the use of 3D plots (weight gain surfaces). The typical $w - t - T$ (temperature) diagram is presented in Fig. 5a, and it is obvious that the 700 °C TGA curve appears as a ridge on the w surface corresponding to an oxygen pressure of 1.3 kPa. The analogous situation is also observed in the $w - t - \lg p_{O_2}$ (oxygen pressure) diagrams, for example, at 800 °C a ridge lies at a pressure of about 13 kPa (Fig. 5b). A ridge violates the monotonicity property of the obtained kinetics phenomenological model in the parameter ranges. Therefore, these ridge temperatures of about 700–800 °C and/or ridge oxygen pressures of about 1.3–13 kPa serve as clearly visible boundaries between different behaviour of the material and prevailing oxidation mechanisms, which are observed due to different combinations of oxidation parameters.

3.2. Carbon burn-off kinetics

A TGA curve of the oxidation of HMC samples, as well as those for titanium carbide or other transition-metal refractory carbides, is influenced by two concurrent processes with opposite effects on the weight of the sample:

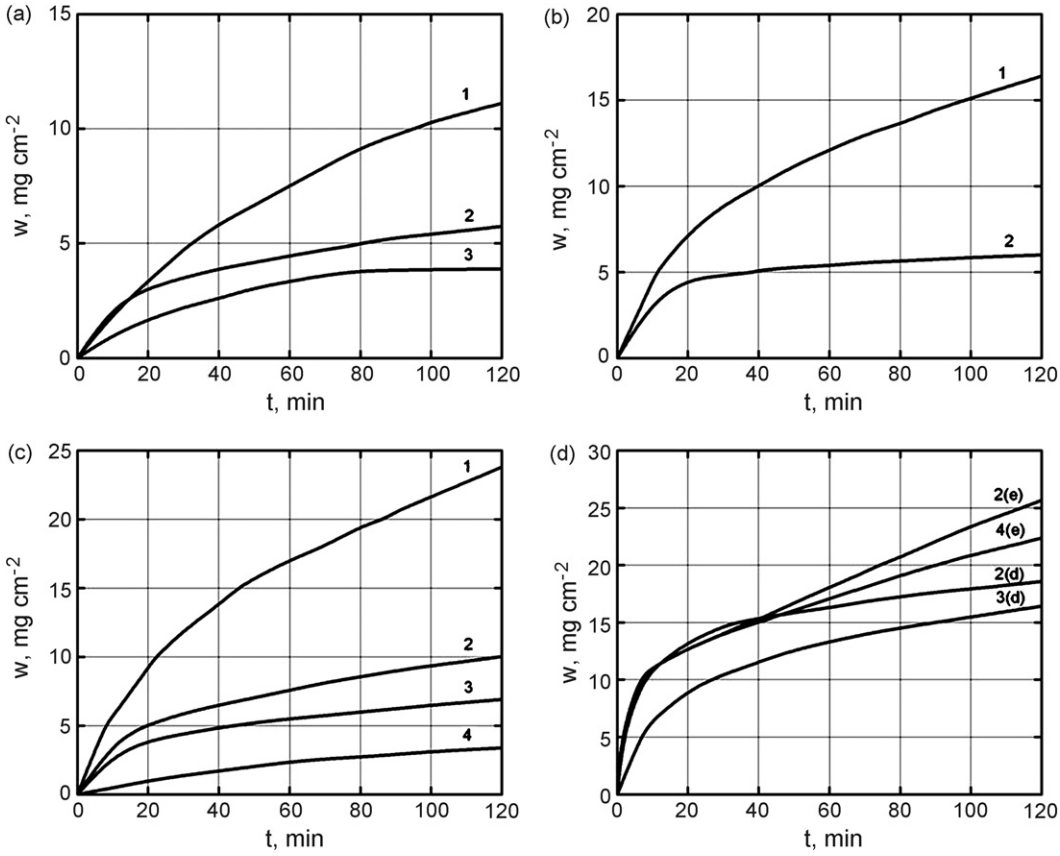

Fig. 3. The isobaric–isothermal oxidation TGA kinetics of 93 vol.% TiC–7 vol.% C HMC at different oxygen pressures, p_{O_2}: (a) 0.13 kPa; (b) 0.65 kPa; (c) 1.3 kPa; (d) 26 kPa; (e) 65 kPa for higher temperatures, T: (1) 700 °C; (2) 800 °C; (3) 900 °C; (4) 1000 °C.

- the formation of titanium (metal) oxycarbides/oxides accompanied by a weight gain[3,9–11,35] and
- the formation of carbon oxides accompanied by a weight loss.

The similar situation is quite often observed during the oxidation of ceramic matrix composites, when simultaneous processes are acting in differing directions.[41] In this case TGA curves possess an inherent uncertainty in relation to real chemical reactions, which contribute to the oxidation process of the composite in general. It is known that titanium carbide like other refractory carbides and compositions based on them does not oxidise with the same characteristic C/Me ratio detected in the initial composition before oxidation.[20–22,33] That is why it was very important to determine the evolution of carbon burn-off during the oxidation of the TiC–C HMC in order to obtain accurate data on the oxygen consumption of the solid for dissolution and scale growth processes, and then evaluate the influence of the above mentioned uncertainty on the values of the output parameters of the kinetics phenomenological model.

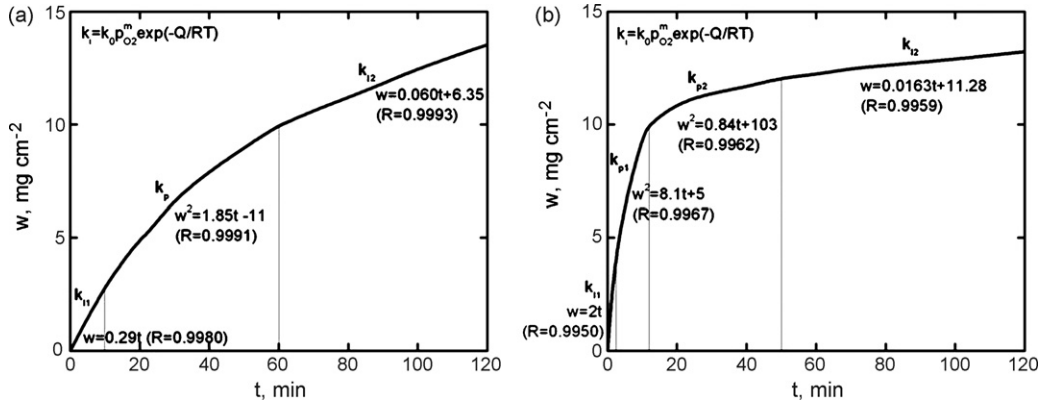

Fig. 4. The scheme of the linear–paralinear model for the oxidation process of 93 vol.% TiC–7 vol.% C HMC: (a) lower temperatures and higher temperatures/lower oxygen pressures, e.g. $T = 600$ °C and $p_{O_2} = 13$ kPa; (b) higher temperatures/higher oxygen pressures, e.g. $T = 700$ °C and $p_{O_2} = 26$ kPa.

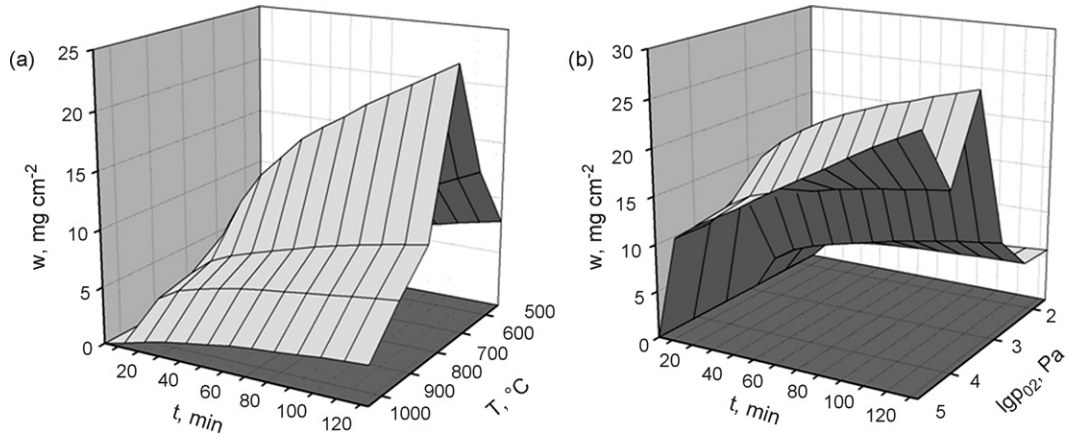

Fig. 5. "Ridge effect" plots showing the influence of temperature T and oxygen pressure p_{O_2} on the oxidation kinetics $w = f(t)$ of 93 vol.% TiC–7 vol.% C HMC at different values of these parameters: (a) $p_{O_2} = 1.3$ kPa; (b) 800 °C.

Thus, by means of a chemical analysis of carbon content for samples exposed to different oxidation conditions, it became possible to establish that the carbon burn-off relationship effectively follows the parabolic rate rule:

$$\left(\frac{\Delta m_C}{s}\right)^2 = k_{pC}t + c_{pC} \tag{3}$$

where Δm_C is the mass (weight) of carbon burnt-off over time t, for a sample with surface area s, k_{pC} and c_{pC} are the parabolic rate constants. Fig. 6 shows the plots of $(\Delta m_C/s)^2$ versus t for the carbon burn-off kinetics at different temperatures and pressures. It seems likely that this relationship describes the oxidation behaviour of many carbon-containing compositions over a wide range of oxidation parameters, T and p_{O_2} with rates of carbon burn-off ranging from 0.05 to 16 mg cm^{-2}. This parabolic rate equation also provides good agreement on carbon burn-off kinetics in the case of the oxidation of quite different compositions of HMC at higher temperatures, e.g. 51 vol.% TiC–19 vol.% TiB_2–30 vol.% C (Fig. 6d).

3.3. Oxygen consumption kinetics

The determination of weight loss due to the formation of carbon oxides allows to convert the results of TGA into oxygen consumption data, generating kinetics curves for surface scale formation, as in general the value of w, observed during the oxidation process by TGA, is given by

$$w = \frac{\Delta m_O - \Delta m_C}{s} \tag{4}$$

where Δm_O is the mass (weight) of oxygen consumed during the dissolution and scale growth processes. Some examples of the calculated kinetic curves for oxygen consumption (plots of $\Delta m_O/s$ versus t) are presented jointly with experimental curves for carbon burn-off in Fig. 7. As expected, oxygen consumption obeys the parabolic rate rule during the parabolic stages of oxidation process, so that

$$\left(\frac{\Delta m_O}{s}\right)^2 = k_{pO}t + c_{pO} \tag{5}$$

where k_{pO} and c_{pO} are the corresponding rate constants. The plots of $(\Delta m_O/s)^2$ versus t (Fig. 8) clearly illustrate the transitions from linear to parabolic forms of the oxidation rate equation and the transitions between the two parabolic stages at higher temperatures/higher pressures as well as confirm good correspondence with those points on the TGA kinetics curves.

3.4. Oxygen pressure effect

The effects of gas pressure on the solid–gas interaction kinetics is one of the most important factors in improving understanding of the interaction mechanism. Some examples of the plots of $\lg k_i$ versus $\lg p_{O_2}$ for k_{l1}, k_p, k_{p1}, k_{p2}, k_{l2} are shown in Fig. 9 to illustrate the influence of oxygen pressure on oxidation rate. These relationships, over a wide range of studied temperatures and oxygen pressures, can be described by a simple equation of the form:

$$\lg k_i = m \lg p_{O_2} + a \tag{6}$$

The calculated values of m across the studied range of oxidation parameters have been collected together in Table 4. Inflection points in these plots are clearly observable as a change of sign of the exponent m (the order of reaction) in the above equation. These negative values for m were revealed in the range of lower temperatures/higher pressures for the most part during stages of linear–paralinear oxidation. This is an interesting result given that after a ridge oxygen pressure has been reached, the oxidation rates of the sample compositions are decreased by further increase in oxygen pressure. Similar trends were observed by Shimada and Kozeki[18] for the isothermal oxidation of TiC_{1-x} powders at 400 °C at oxygen pressures higher than 7.9 kPa. Gozzi et al.[29] also reported about decrease of oxidation rate with growing of oxygen partial pressure at 1000 °C from 9 to 19 Pa, approximately corresponding with $m = -3/4$. Another key characteristic of this process, observed for both linear and

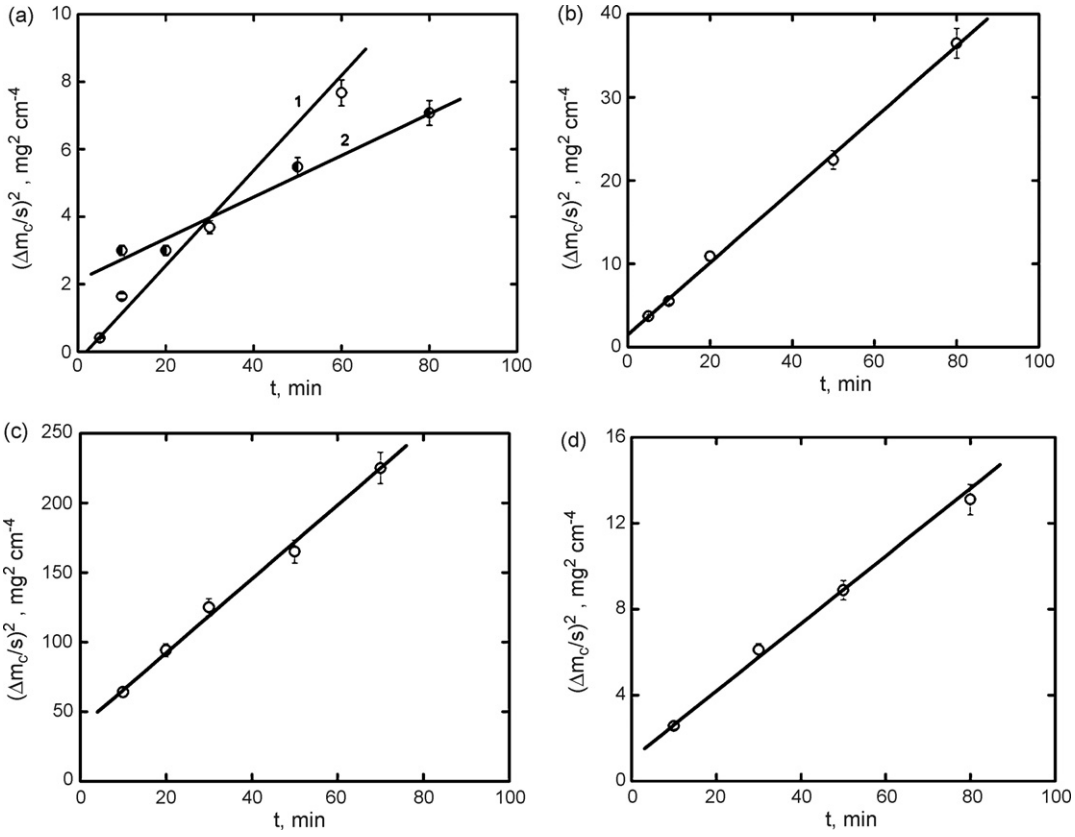

Fig. 6. Plots of $(\Delta m_C/s)^2$ vs. t for the carbon burn-off kinetics during the oxidation of HMC: (a–c) 93 vol.% TiC–7 vol.% C and (d) 51 vol.% TiC–19 vol.% TiB_2–30 vol.% C at different oxygen pressures: (a1 and b) $p_{O_2} = 1.3$ kPa; (a2, c and d) $p_{O_2} = 13$ kPa and temperatures: (a) $T = 500\,^{\circ}$C; (b) and (c) $T = 700\,^{\circ}$C; (d) $T = 900\,^{\circ}$C.

parabolic stages, is the gradual increase of the absolute value of m with an increase of oxidation temperature for the TiC–C HMC: from $m = 0 - 1/3$ at 500 °C and $m = 1/10 - 1/2$ at 600 °C up to $m = 1/3 - 1/2$ at 900 °C and $m = 1/2 - 1$ at 1000 °C, as for TiC_{1-x} powder Stewart and Cutler[15] reported about $m = 1/6$ at 750–800 °C and $m = 1/4$ at 800–900 °C. It is necessary to note that the application of Eq. (5) for oxygen consumption kinetics, at the same temperatures and oxygen pressures, gives approximately the same values for m as those determined for the TGA kinetics (see Fig. 9).

3.5. Temperature effect

Preliminary inspection of the experimentally obtained w versus t plots suggests a clear dependence of oxidation rate on temperature, although this rate tends to rise to a maximum at the ridge temperature before falling with further temperature increases. The Arrhenius plots of $\ln k_i$ versus $1/T$ for the different stages of the process at oxygen pressures from 0.13 up to 13 kPa are shown in Fig. 10. For temperatures below the ridge temperature of 700 °C, the Arrhenius plot behaviour is typi-

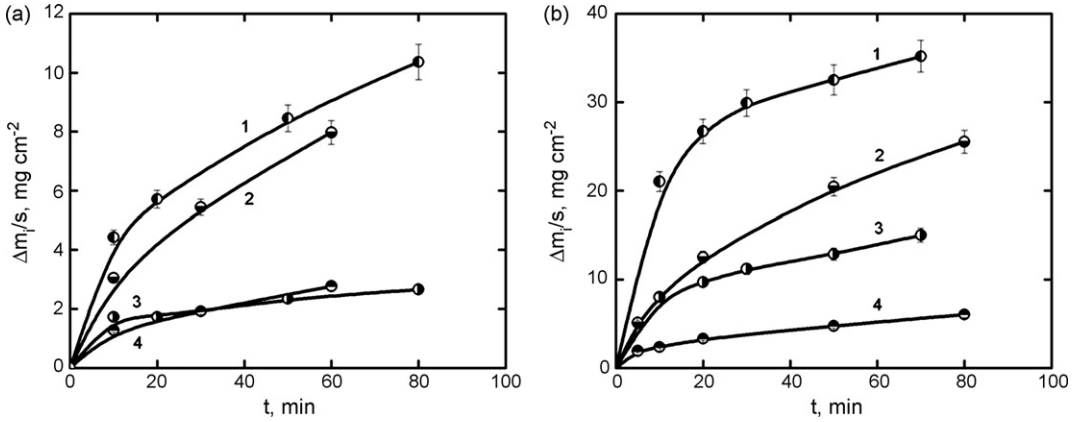

Fig. 7. The oxygen consumption (1 and 2) and carbon burn-off (3 and 4) kinetics during the oxidation of 93 vol.% TiC–7 vol.% C HMC at temperatures: (a) $T = 500\,^{\circ}$C; (b) $T = 700\,^{\circ}$C and oxygen pressures: (2 and 4) $p_{O_2} = 1.3$ kPa; (1 and 3) $p_{O_2} = 13$ kPa.

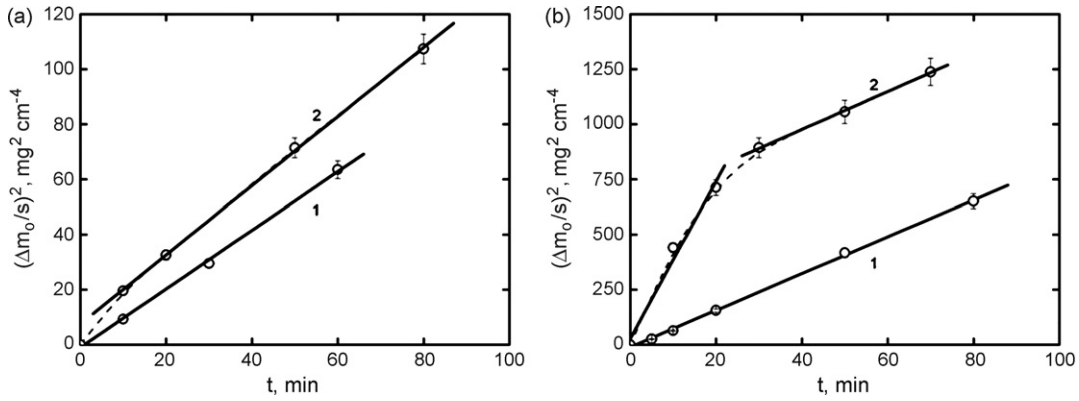

Fig. 8. Plots of $(\Delta m_O/s)^2$ vs. t for the oxygen consumption (dissolution and scale growth) kinetics during the oxidation of 93 vol.% TiC–7 vol.% C HMC at temperatures, T: (a) 500 °C; (b) 700 °C and oxygen pressures, p_{O_2}: (1) 1.3 kPa; (2) 13 kPa.

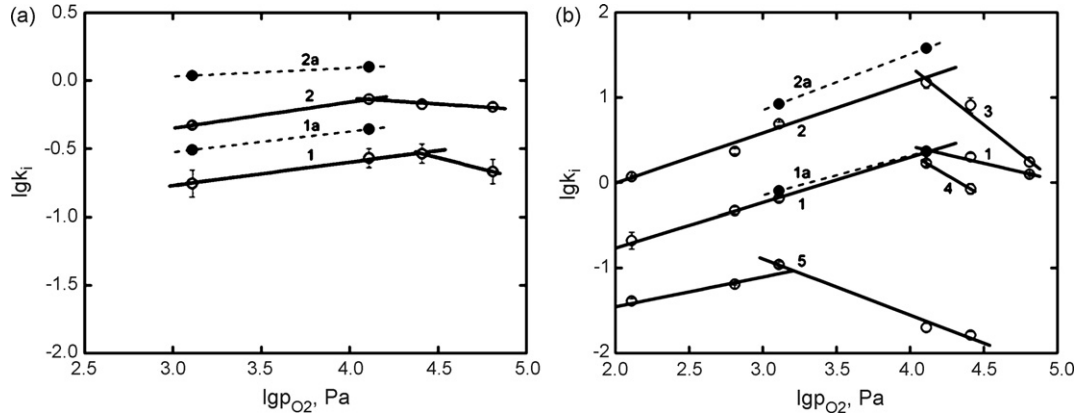

Fig. 9. Relationship between lg k_i for rate constants (1) k_{l1}, (2) k_p, (3) k_{p1}, (4) k_{p2}, (5) k_{l2} and oxygen pressures lg p_{O_2} during the oxidation of 93 vol.% TiC–7 vol.% C HMC at different temperatures, T: (a) 500 °C; (b) 700 °C (curves with indices 1a and 2a relate to oxygen consumption kinetics).

cal, in that the rate of oxidation of the material increases with temperature. Within the range of higher temperatures, the same behaviour was found at the lowest oxygen pressure, but only for the initial stage of oxidation (see Fig. 10a). For low oxygen pressures in the temperature interval from 700 to 1000 °C, the rate of oxidation for the material is generally slowed with an increase of temperature. At the ridge temperature in the plot of ln k_i versus $1/T$ there is an inflexion point (see Fig. 10c), at which the activation energy Q in the conventional equation:

$$k_i = k_{0i} p_{O_2}^m \exp\left(-\frac{Q}{RT}\right) \quad (7)$$

Table 4
The calculated values of reaction order m at different temperatures and oxygen pressures[a]

m	0.13–0.65 kPa	0.65–1.3 kPa	1.3–13 kPa	13–26 kPa	26–65 kPa
500 °C	–		1/6 / 1/5-1/6 / 0	1/6 / –1/10 / 0	–⅓ / –1/10 / 0
600 °C	–	1/5-1/6 / ⅓ / 1/6-1/10		1/5-1/6 / –½ / 1/6-1/10	
700 °C	½ / ½ / ⅓		½ / ½ / –(½-⅔)	–(½-⅓) / –1 / –(½-⅔)	
800 °C	½ / ½ / ⅓			½ / –1-0 / ⅓	
900 °C	½-⅓ / ½ / ⅓				–
1000 °C	–		1 / 1 / ½		

[a] Light grey areas provide the values of m and the dark grey regions represent negative m values for $k_{l1}/k_p/k_{l2}$ in the relationships $k_i \sim p_{O_2}^m$; white boxes represent regions where no data has been taken.

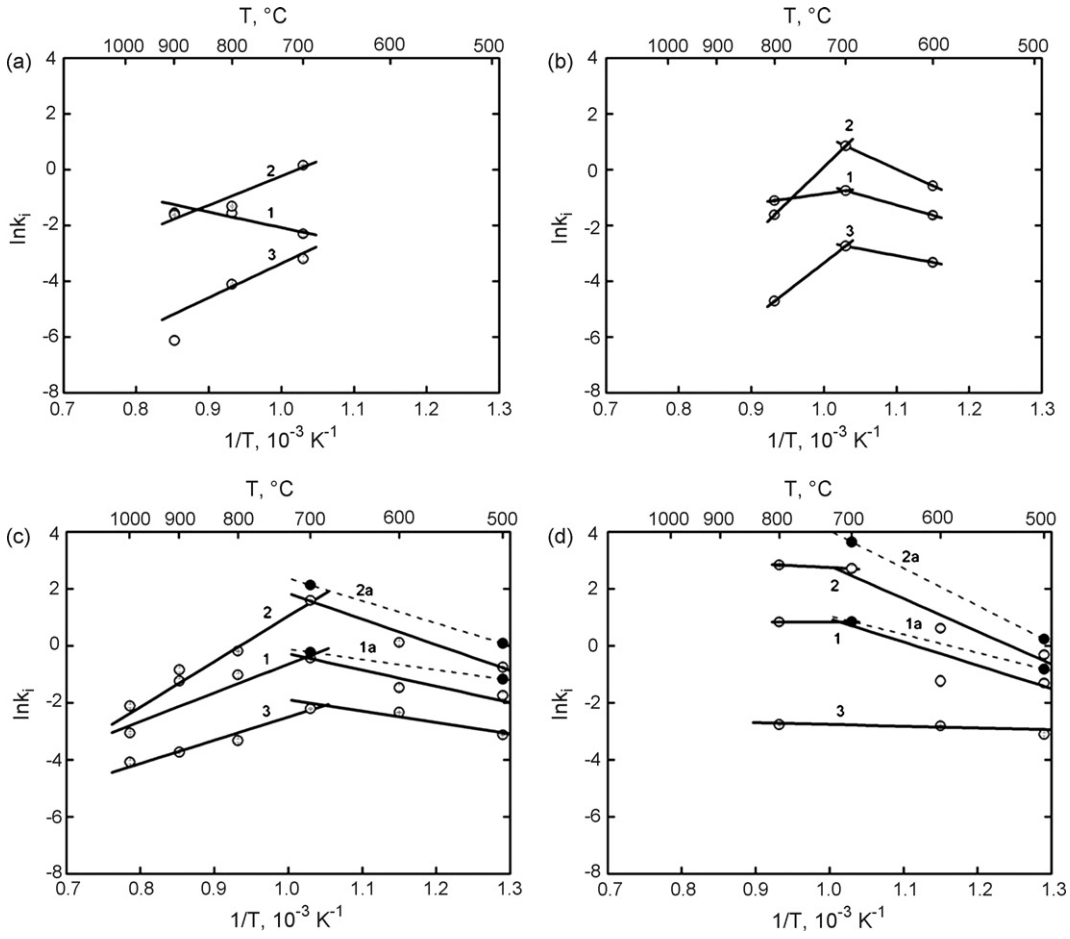

Fig. 10. Arrhenius plots of $\ln k_i$ for rate constants (1) k_{l1}, (2) k_p, (3) k_{l2} vs. $1/T$ for the oxidation of 93 vol.% TiC–7 vol.% C HMC at different oxygen pressures, $\lg p_{O_2}$: (a) 0.13 kPa; (b) 0.65 kPa; (c) 1.3 kPa; (d) 13 kPa (curves with indices 1a and 2a relate to oxygen consumption kinetics).

where k_{0i} is a pre-exponential constant (independent of oxidation parameters), changes sign as was found for the inflection point at the ridge pressure of oxygen for Eq. (6), where the order of reaction m also changed its sign in the same manner. Comparison of the $\ln k_i$ versus $1/T$ plots, obtained from the oxygen consumption kinetics data, with those from the TGA, as demonstrated by Fig. 10c and d, shows that these two types of data are in good agreement with each other. At oxygen pressures from

Table 5
The calculated values of activation energy Q at different temperatures and oxygen pressures[a]

Q, kJ mol^{-1}	500–600 °C	600–700 °C	700–800 °C	800–900 °C	900–1000 °C
0.13 kPa	–		46±8 / –(87±2) / –(102±6)		–
0.65 kPa	–	61±8 / 99±6 / 41±5	–(30±8) / –(210±10) / –(170±10)	–	
1.3 kPa	47±3 / 75±1 / 33±1		–(84±2) / –(132±2) / –(68±2)		
13 kPa	67±5 / 96±5 / 5±1		0 / 11±6 / 5±1	–	
26 kPa	61±3 / 79±5 / 5±1		61±3 / 0 / 5±1	–	
65 kPa	70±3 / 84±2 / 9±1		0 / 22±6 / 15±6 / 9±1 [b]		

[a]Light grey areas provide the values of Q and the dark grey regions represent negative Q values for $k_{l1}/k_p/k_{l2}$; white boxes represent regions where no data has been taken.
[b]For $k_{l1}/k_{p1}/k_{p2}/k_{l2}$.

26 to 65 kPa the situation is similar; as the Arrhenius plots show a change in gradient at the ridge temperature, but only without a change of the sign for Q. After this ridge temperature, the values of the activation energy Q dramatically drop, as the gradient occasionally falls to near zero. The calculated values of the activation energy Q for the different stages and parameters of oxidation are presented in Table 5.

In summarising the kinetics data, a number of observations on the oxidation process of the TiC–C HMC samples can be made:

- for the initial linear stage, the activation energy Q is 46–70 kJ mol^{-1} throughout the range of oxidation parameters, with the exception of 700–1000 °C at oxygen pressures from 0.65 to 1.3 kPa, where Q is negative and has values between 30 and 84 kJ mol^{-1};
- for the parabolic stages, the activation energy Q is 75–100 kJ mol^{-1} at 500–700 °C (independent of oxygen pressure) and 11–22 kJ mol^{-1} at 700–1000 °C over the range of oxygen pressures from 13 to 65 kPa, except for the higher temperature/lower oxygen pressure range, where Q is negative and has values between 87 and 220 kJ mol^{-1};
- for the final linear stage, the activation energy Q is 33–41 kJ mol^{-1} at 500–700 °C for oxygen pressures of 0.65–1.3 kPa and 5–9 kJ mol^{-1} at higher oxygen pressures (13–65 kPa), except for the higher temperature/lower oxygen pressure range, where Q is negative and has values between 68 and 170 kJ mol^{-1}.

As a result of this kinetic analysis, it becomes possible to divide the studied range of temperatures and oxygen pressures into four main regions; each region defined by high or low values of oxidation parameters (Fig. 11). The ridge temperature and ridge oxygen pressure serve as boundaries for these regions and mark a change in the prevailing oxidation mechanism; a more detailed treatment of changes in these mechanisms will be considered in the next part of this work, supported by additional studies of physico-chemical particularities of the studied process, different phase transformations and transitions occurred in the oxidised HMC samples corresponding to the linear–paralinear phenomenological kinetics model above considered.

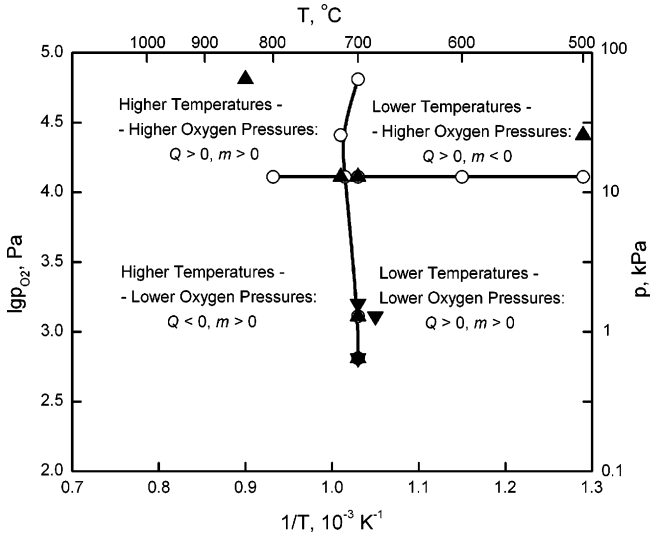

Fig. 11. An oxidation parameter plot of lg p_{O_2} vs. $1/T$ for the oxidation of 93 vol.% TiC–7 vol.% C HMC; each inflexion point, at ridge temperatures/ridge oxygen pressures for different kinetics stages, has been marked as: (◯) parabolic (k_p and k_{p1}); (▲) first linear (k_{l1}); (▼) second linear (k_{l2}).

4. Conclusions

This part of work has been a study of the oxidation kinetics of hot-pressed hetero-modulus ceramic composite materials (HMC), 93 vol.% TiC–7 vol.% C (graphite) at temperatures of 500–1000 °C and pressures of 0.13–65 kPa in an oxygen flow with a rate of about 0.1 g min^{-1}. A number of conclusions can be drawn concerning the oxidation behaviour of this material within the frames of developed kinetics phenomenological model:

(1) The formal process kinetics, namely the evolution of weight gain obtained using TGA, can be described by a multi-stage, linear–paralinear model: the first stage is governed by linear kinetics, the subsequent (main) stage by the parabolic rate equation and, the final stage by a return to a linear form. At higher temperatures/higher oxygen pressures, it was necessary to treat the main parabolic stage as two separate parabolic stages (instead of one) with different kinetics constants.

(2) Experimentally it was shown first for transition-metal carbides and carbide-containing compositions that the carbon burn-off kinetics observed during the main stage of the process follows a parabolic reaction rate equation. The oxygen consumption (dissolution and scale growth) kinetic constants, determined from TGA and carbon burn-off analysis, confirmed that both types of kinetics phenomenological models (TGA and oxygen consumption) produce approximately the same values of output parameters: activation energy Q and order of reaction m.

(3) The isobaric–isothermal TGA of oxidation process identified the so-called "ridge effect" as the influence of both temperature and oxygen pressure on the rate of oxidation (weight gain per unit surface). The rate increases with the increase of oxidation parameter (temperature or oxygen pressure) up to the values corresponding to the ridge; after this feature, the oxidation rate decreases in spite of the continuing increase of oxidation parameter. In the studied range, ridges were detected for temperatures of about 700–800 °C and oxygen pressures of about 1.3–13 kPa. While traversing the ridge parameter, the values of Q and m in the kinetics relationships vary in value as well as changing their sign.

(4) Employing isobaric–isothermal TGA and carbon content chemical analysis it became possible to divide the studied range of temperatures and oxygen pressures into four main regions; each region defined by high or low values of oxidation parameters. The ridge temperature and ridge oxygen pressure serve as boundaries for these regions and mark a change in the prevailing oxidation mechanism.

Acknowledgements

The authors wish to thank Prof. A.R. Beketov, Ural State Technical University, Russia and Prof. G.M. Romantsev, Russian State Professional and Pedagogical University for providing the necessary technological and research facilities and would like to express their gratitude to Prof. D.K. Ross for support and assistance in the preparation this work for publication.

References

1. Hasselman, D. P. H., Becher, P. F. and Mazdiyasni, K. S., Analysis of the resistance of high-E, low-E brittle composites to failure by thermal shock. *Z. Werkstofftech.*, 1980, **11**(3), 82–92.
2. Mazdiyasni, K. S. and Ruh, R., High/low modulus Si_3N_4–BN composite for improved electrical and thermal shock behaviour. *J. Am. Ceram. Soc.*, 1981, **64**(7), 415–419.
3. Shabalin, I. L., Beketov, A. R., Vlasov, V. G. and Rozhkov, A. S., Oxidation of the titanium carbide–carbon composites at 500–1000 °C. In *Refractory Compounds*, ed. P. S. Kyslyi. Ukrainian SSR Academy of Science Institute for Problems of Materials Science, Kiev, 1981, pp. 129–132.
4. Shabalin, I. L., Beketov, A. R., Gorinskii, S. G., Podkovyrkin, M. I. and Fedorenko, O. V., Study of strength characteristics of titanium carbide–silicon carbide–carbon hot-pressed materials. In *Alloys of Refractory and Rare Metals for High-Temperature Application. Proceedings of the All-USSR Conference on Physico-Chemical Principles of Development for Heat-Resisting Metal Materials*, ed. E. M. Savitskii, 1984, pp. 186–189.
5. Grushevskii, Ya. L., Frolov, V. F., Shabalin, I. L. and Cheboryukov, A. V., Mechanical behaviour of the ceramics containing boron nitride. *Sov. Powder Metall. Met. Ceram.*, 1991, **30**(4), 338–341.
6. Zhukov, Yu. N., Cherepanov, A. V., Beketov, A. R. and Shabalin, I. L., Inspection of the nonuniformity of a ceramic compact for machining by hardness measurement. *Sov. Powder Metall. Met. Ceram.*, 1991, **30**(4), 349–351.
7. Shabalin, I. L., Tomkinson, D. M. and Shabalin, L. I., High-temperature hot-pressing of titanium carbide–graphite hetero-modulus ceramics. *J. Eur. Ceram. Soc.*, 2007, **27**(5), 2171–2181.
8. Araki, M., Sasaki, M., Kim, S., Suzuki, S., Nakamura, K. and Akiba, M., Thermal response experiments of SiC/C and TiC/C functionally gradient materials as plasma facing materials for fusion application. *J. Nucl. Mater.*, 1994, **212–215**, 1329–1334.
9. Kuptsov, S. G., Vlasov, V. G., Beketov, A. R., Shabalin, I. L., Fedorenko, O. V. and Pykhteev, Yu. P., Low-temperature oxidation mechanism of zirconium carbide. In *Kinetics and Mechanism of Reactions in Solid State*, ed. E. A. Prodan. Byelorussian State University, Minsk, 1975, pp. 182–183.
10. Vlasov, V. G., Alabushev, V. A. and Beketov, A. R., Oxidation of solid solutions of uranium and niobium monocarbides. *Sov. Atom. Energy*, 1975, **38**(6), 539–542.
11. Afonin, Yu. D., Shalaginov, V. N. and Beketov, A. R., High-temperature oxidation of niobium monocarbide. *J. Appl. Chem. USSR*, 1985, **58**(3 Pt. 1), 423–427.
12. Samsonov, G. V. and Golubeva, N. K., Some rules and the mechanism of the oxidation of high-melting titanium compounds. *J. Phys. Chem. USSR*, 1956, **30**(6), 1258–1266.
13. Webb, W. W., Norton, J. T. and Wagner, C., Oxidation studies in metal–carbon systems. *J. Electrochem. Soc.*, 1956, **103**(2), 112–117.
14. Macdonald, N. F. and Ransley, C. E., The oxidation of hot-pressed titanium carbide and titanium boride in the temperature range 300–1000 °C. *Powder Metall.*, 1959, **3**, 172–176.
15. Stewart, R. W. and Cutler, I. V., Effect of temperature and oxygen partial pressure on the oxidation of titanium carbide. *J. Am. Ceram. Soc.*, 1967, **50**(4), 176–180.
16. Reichle, M. and Nickl, J. J., Untersuchungen über die Hochtemperaturoxidation von Titankarbid. *J. Less-Common Met.*, 1972, **27**, 213–236.
17. Lavrenko, V. A., Glebov, L. A., Pomitkin, A. P., Chuprina, V. G. and Protsenko, T. G., High-temperature oxidation of titanium carbide in oxygen. *Oxide Met.*, 1975, **9**(2), 171–179.
18. Shimada, S. and Kozeki, M., Oxidation of TiC at low temperatures. *J. Mater. Sci.*, 1992, **27**(7), 1869–1875.
19. Shimada, S., A thermoanalytical study of oxidation of TiC by simultaneous TGA–DTA–MS analysis. *J. Mater. Sci.*, 1996, **31**(3), 673–677.
20. Shimada, S., Yunazar, F. and Otani, S., Oxidation of hafnium carbide and titanium carbide single crystals with the formation of carbon at high temperatures and low oxygen pressures. *J. Am. Ceram. Soc.*, 2000, **83**(4), 721–728.
21. Shimada, S., Hayashi, S. and Yunazar, F., High temperature oxidation of $(Ti_{0.5}Hf_{0.5})C$ ceramics fabricated by hot-pressing. *J. Ceram. Soc. Jpn.*, 2002, **110**(1279), 167–172.
22. Johnsson, M. and Shimada, S., Oxidation of $Ta_xTi_{1-x}C$ whiskers under formation of carbon. *J. Mater. Sci. Lett.*, 2002, **21**(12), 955–958.
23. Shimada, S. and Mochidsuki, K., The oxidation of TiC in dry oxygen, wet oxygen, and water vapor. *J. Mater. Sci.*, 2004, **39**(2), 581–586.
24. Onuma, A., Kiyono, H., Shimada, S. and Desmaison, M., High temperature oxidation of sintered TiC in an H_2O-containing atmosphere. *Solid State Ionics*, 2004, **172**(1–4), 417–419.
25. Shimada, S., Onuma, T., Kiyono, H. and Desmaison, M., Oxidation of HIPed TiC ceramics in dry O_2, wet O_2, and H_2O atmospheres. *J. Am. Ceram. Soc.*, 2006, **89**(4), 1218–1225.
26. Gozzi, D., Guzzardi, G., Montozzi, M. and Cignini, P. L., Kinetics of high temperature oxidation of refractory carbides. *Solid State Ionics*, 1997, **101–103**(2), 1243–1250.
27. Cignini, P. L. and Gozzi, D., Weak interaction of oxygen with refractory carbides. In *Proceedings of the Symposium on High Temperature Corrosion and Materials Chemistry*. Electrochemical Society, Pennington, 1998, pp. 349–365.
28. Gozzi, D., Montozzi, M. and Cignini, P. L., Apparent oxygen solubility in refractory carbides. *Solid State Ionics*, 1999, **123**(1), 1–10.
29. Gozzi, D., Montozzi, M. and Cignini, P. L., Oxidation kinetics of refractory carbides at low oxygen partial pressures. *Solid State Ionics*, 1999, **123**(1), 11–18.
30. Gozzi, D., Cascino, G., Loreti, S., Minarini, C. and Shimada, S., Weak interaction of oxygen with some refractory carbides. *J. Electrochem. Soc.*, 2001, **148**(4), J15–J24.
31. Bellucci, A., Di Pascasio, F., Gozzi, D., Loreti, S. and Minarini, C., Structural characterization of TiO_2 films obtained by high temperature oxidation of TiC single crystals. *Thin Solid Films*, 2002, **405**(1/2), 1–10.
32. Bellucci, A., Gozzi, D., Kimura, T., Noda, T. and Otani, S., Auger electron spectroscopy analysis of cross-section surface of oxidized titanium carbide single crystal. *J. Am. Ceram. Soc.*, 2003, **86**(12), 2116–2121.
33. Bellucci, A., Gozzi, D., Nardone, M. and Sodo, A., Rutile growth mechanism on TiC monocrystals by oxidation. *Chem. Mater.*, 2003, **15**(5), 1217–1224.
34. Bellucci, A., Gozzi, D. and Latini, A., Overview of the TiC/TiO_2 (rutile) interface. *Solid State Ionics*, 2004, **172**(1–4), 369–375.
35. Afonin, Yu. D., Shalaginov, V. N. and Beketov, A. R., High-temperature oxidation of carbide–carbon materials of the NbC–C and NbC–TiC–C systems. *J. Appl. Chem. USSR*, 1981, **54**(4), 625–628.
36. McNally, R. N. and Bardhan, P., Oxidation resistance of fused TiC–C compositions containing chromium. *J. Mater. Sci.*, 1983, **18**(4), 1213–1223.
37. Kostikov, V. I., Racoch, A. G., Kravetskii, G. A., Airapetov, B. L., Pososeva, G. D., Drugov, P. N. *et al.*, Influence of heating procedure on the process of high-temperature oxidation in carbide–graphite composite materials. *Inorg. Mater.*, 1981, **17**(3), 352–354.
38. Afonin, Yu. D., Thermogravimetric unit for studies of gas–solid body interaction processes. *J. Phys. Chem. USSR*, 1976, **50**(8), 2156–2157.
39. Afonin, Yu. D., Shalaginov, V. N. and Beketov, A. R., Communications interface for the Elektronika DZ-28 microcomputer and experimental equipment. *Instrum. Exp. Tech.*, 1984, **27**(6/1), 1374–1377.
40. Voitovich, R. F. and Pugach, E. A., High-temperature oxidation of titanium carbide. *Sov. Powder Metall. Met. Ceram.*, 1972, **11**(2), 132–136.
41. Nickel, K. G., Ceramic matrix composite models. *J. Eur. Ceram. Soc.*, 2005, **25**(10), 1699–1704.